DOI: 10.24352/UB.OVGU-2017-120 TECHNISCHE MECHANIK, 37, 2-5, (2017), 442 – 449
submitted: August 30, 2017

Run-up Simulation of Automatic Balanced Rotors Considering Velocity-dependent Drag Coefficients

L. Spannan, C. Daniel, E. Woschke

The paper at hand presents the modelling approach of a laboratory centrifuge with a vertically mounted rotor and an automatic balancing device, which counterbalances the unbalance in one plane. This device consists of an annulus containing the outer ring of a ball-bearing as well as steel balls and is filled with a newtonian fluid. The fluid, accelerated by the annulus' walls, flows around the balls and positions them in the annulus. In order to develop a design method for the balancing device the velocity dependency of the drag coefficient is considered and the influence of fluid density and viscosity on the balancing efficiency is examined. An experimental comparison shows that the flow in the concave bearing race can be represented by the flow around a ball in contact with a flat surface. It can be shown that, depending on the run-up acceleration, a selective choice of the fluid properties has a positive influence on the vibrations near the critical speed and the response time of the counterbalancing effect at supercritical speeds.

1 Introduction

Unbalances in high-speed rotors can lead to excessive vibrations. At the same time, balancing of unbalances due to production or assembly can be uneconomical or process dependent variations in imbalance may be present. In these cases automatic balancing systems can be implemented, which use movable fluids or solids in order to counterbalance the rotor unbalance. Applications of such systems can be found in CD-ROM drives, washing machines and angle grinders.

It is common knowledge that dynamic systems show a phase shift between excitation and deflection while passing resonances. Assuming low damping, the rotor deflects in the direction of the unbalance when operated subcritically and deflects opposing the unbalance when operated supercritically. In contrast, the balancing masses in automatic balancers are driven speed independently by the centrifugal forces F_{cf} to the position most distant to the center of rotation $\mathcal{O}_R$, meaning in the direction of deflection e of the center of geometry $\mathcal{O}_G$. Therefore, automatic balancers are increasing the unbalance excitation at subcritical speeds and act counterbalancing at supercritical speeds, see fig. 1. In order to get a good description of the transient positioning of the counterbalancing masses the modelling of the driving forces is essential. The aim of this paper is to contribute to this model with regard to the description of flow resistance. Without loss of generality the following explanations and descriptions refer to automatic balancers with one ball only.

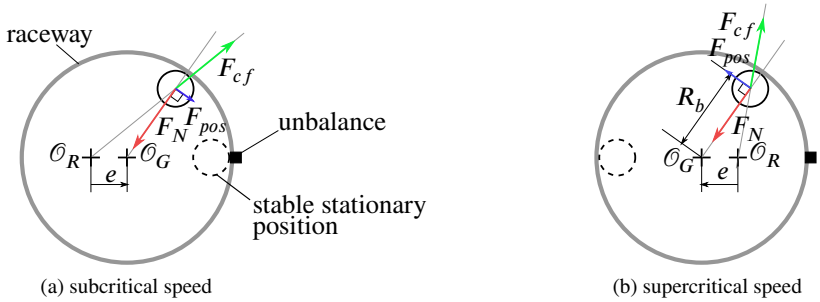

Figure 1: Functionality of automatic ball balancers. Demonstration of driving forces on the counterbalancing mass in a rotating reference frame.

2 State of Research

One of the first publications on ball balancers is the patent from Thearle (1936). Since then, multiple studies were conducted and a growing interest in this topic can be observed, especially in the last 15 years. In order to achieve an efficient balancing device multiple system parameters need to be specified. The findings from preceding publications are summarised in this section.

2.1 Friction

The contact between the balls and the raceway is inducing friction, which is directed oppositely to the ball movement along the raceway. Figure 1 shows that the driving force

$$F_{pos} = |\vec{F}_{pos}| = |\vec{F}_{cf} + \vec{F}_N|, \tag{1}$$

with $\vec{F}_N$ describing the normal force on the ball, is decreasing with increasing approach to the stable stationary position. Therefore, an area near the stable stationary position exists where the friction is sufficient to hold the ball in place aside the ideal position. Hence the optimal counterbalancing cannot be achieved.

This negative influence of friction was identified analytically by Huang et al. (2002). Ishida et al. (2012) used different friction modelling approaches in their numerical models. They differentiated between Coulomb friction, which is proportional to the normal force, static rolling friction and rolling friction on the basis of hysteresis losses and concluded that the static rolling friction is influencing the balancing effectiveness dominantly. With respect to the design of automatic balancing devices a minimisation of the ball and raceway surface roughness is to be aspired. As described by Ishida et al. (2012), the influence of friction can be reduced by an increased number of balls, preferably in separate raceways, because the balls are not getting to rest at the same time. In addition, the static rolling friction decreases with increasing ball diameter.

2.2 Raceway Eccentricity

Due to an eccentricity ϵ of the raceway, its geometric centre $\mathcal{O}_G$ is not coinciding with the center of mass $\mathcal{O}_M$ of the balanced rotor, leading to a stable position ($F_{pos} = 0$) of the ball aside the ideal balancing position, see fig. 2. This negative influence was examined by Huang et al. (2002) and Majewski (1988) amongst others. From this follows that irregularities of the circular race form, see fig. 3, have negative influence on the balancing capabilities, too.

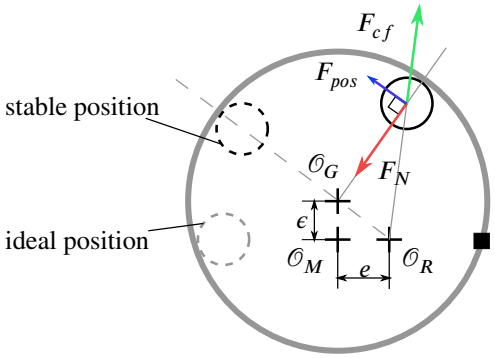

Figure 2: Influence of raceway eccentricity on the positioning at supercritical speeds.

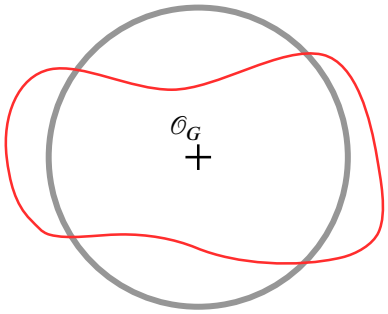

Figure 3: Exaggerated representation of an arbitrary form irregularity.

2.3 Non-synchronous Motions

Ryzhik et al. (2003) showed that in an operation range above the critical speed ω_i the balancing balls are not circulating with the rotor frequency but with the critical frequency. This causes the balls to not come to rest and therefore the rotor unbalance cannot be counterbalanced. Only after reaching a border rotating speed $\Omega_{bo,i}$ the balls get accelerated to the rotor speed resulting in the balancing effect to be performed. In order to avoid the operation

of automatic balancing devices below the critical speed and in the speed range of non-synchronous motions, the operating range has to be restricted, see fig. 4. A possible solution to avoid non-synchronous motions by using multiple balls and partitioning the annulus is described by Ishida et al. (2012). The partitioning walls are enforcing the rotor speed to the balls, avoiding non-synchronous motions. As a drawback, the maximum counterbalancing force is reduced.

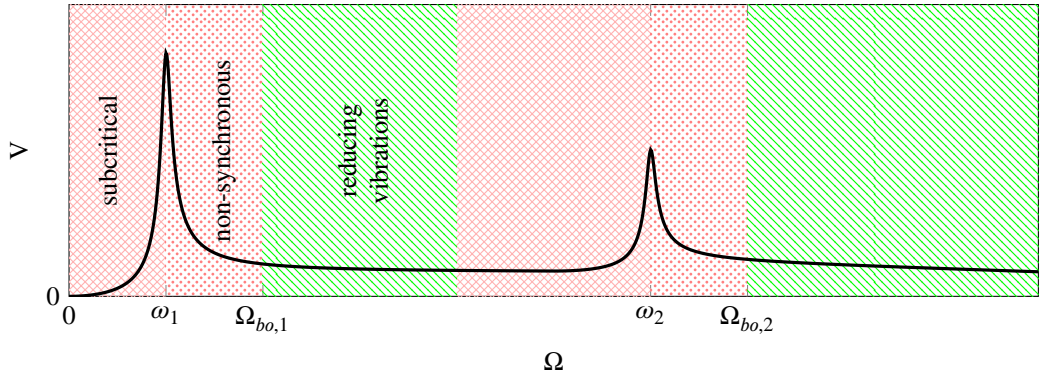

Figure 4: Exemplary magnifying function of an unbalanced rotor with operation ranges of automatic balancing devices.

2.4 Viscosity and Density of the Fluid

In contrast to the surface roughness and the raceway eccentricity, where small values are preferred, the choice of an optimal fluid in the automatic balancing system leads to a conflict of aims (Ryzhik et al. (2003)), which has to be resolved. With increasing density ρ_{fl} and viscosity ν the lag between the rotor and ball velocity is decreased due to the flow resistance. On one hand the lag is desired at subcritical speeds so that the balls are not positioned near the rotor imbalance causing an increase in rotor vibration. On the other hand a fast reduction of lag and positioning of the balls to their ideal position is desired once the critical speed is exceeded. The objective of the choice of fluid is to keep the vibrations in the run-up phase moderate and to gain a quick balancing effect at supercritical speeds. The modelling of the viscous coupling between the rotor (the annulus), the fluid and the balls has a great impact on the quality of the simulation results.

Many previous stationary (Ryzhik et al. (2003); Green et al. (2006); Ishida et al. (2012); Kim and Na (2013); Chen and Zhang (2016)) and transient (Sperling et al. (2002)) models make use of a linear correlation between the moment of fluid drag M_D and the difference in rotating speed between the rotor and the ball

$$M_D = \beta \cdot \left(\dot{\varphi}_R - \dot{\varphi}_b\right). \tag{2}$$

The parameter β inherits several system properties and depends on the fluid, the annulus geometry and the ball diameter and is difficult to determine without experimental data. Huang et al. (2002) make use of a physically motivated approach on the basis of the fluid drag force F_D, leading to a nonlinear correlation between the moment and the rotating speed difference based on geometric and physical quantities

$$M_D = F_D \cdot R_b = \frac{1}{2}\rho_{fl} \cdot \bar{A} \cdot C_D \cdot v_{rel}^2 \cdot R_b \cdot \mathrm{sign}(v_{rel}) \tag{3}$$

$$= \underbrace{\frac{1}{2}\rho_{fl} \cdot \bar{A} \cdot R_b^3}_{constant} \cdot C_D \cdot \left(\dot{\varphi}_R - \dot{\varphi}_b\right)^2 \cdot \mathrm{sign}(\dot{\varphi}_R - \dot{\varphi}_b). \tag{4}$$

$R_b, \bar{A}, C_D, v_{rel}$ describe the radius of the ball center track, the ball cross-sectional area, the drag coefficient and the flow velocity, respectively. Huang et al. make the assumption of a constant drag coefficient C_D, which is called into question by the authors. Furthermore, it should be noted that the velocity of the fluid $\dot{\varphi}_{fl}$ is not equal to the rotor speed $\dot{\varphi}_R$ in transient models. The spin-up of fluids in rotating annuli cannot be calculated analytically (Benton and Clark (1974)). Hence the fluid is modelled as a rigid body and its acceleration is described by a linear correlation in the style of equation (2)

$$M_{fl} = \beta_{fl}\left(\dot{\varphi}_R - \dot{\varphi}_{fl}\right), \tag{5}$$

where the parameter β_{fl} is fitted to the experimental data. Additionally, the radial increase of the flow velocity, see fig. 5, is neglected for small ball diameters $d << R_b$, leading to a flow velocity of $v_{rel} = R_b(\dot{\varphi}_{fl} - \dot{\varphi}_b)$.

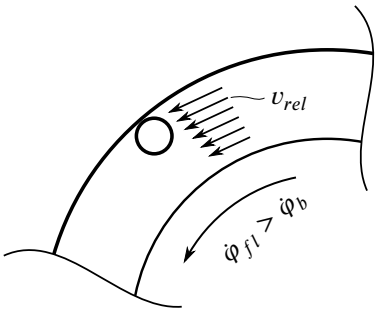

Figure 5: Flow velocity profile at stationary state.

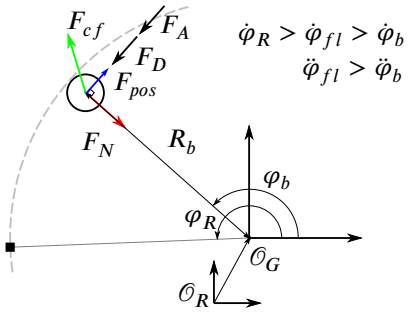

Figure 6: Coordinates and forces describing the dynamics of the balancing ball neglecting raceway eccentricity.

Another aspect of transient modelling is the added virtual mass, whose inertia is antagonising the acceleration of a rigid body in a fluid. The appropriate virtual mass coefficient for balls in contact with a flat surface was identified experimentally by Jan and Chen (1997) to be $C_A = 2$. Derived from their conclusions, the impact of the added mass effect is decreasing with an increasing ratio in the densities ρ_b/ρ_{fl}. The moment of virtual mass equals

$$M_A = F_A \cdot R_b = \rho_{fl} \cdot \frac{\pi d^3}{6} \cdot C_A \cdot \left(\ddot{\varphi}_{fl} - \ddot{\varphi}_b\right) \cdot R_b \,. \tag{6}$$

The recited publications neglect the dependency of the drag coefficient C_D from the flow velocity v_{rel}. This relation is usually expressed with the use of the dimensionless Reynolds number

$$\mathrm{Re} = \frac{v_{rel} \cdot d}{\nu} = \frac{\left(\dot{\varphi}_{fl} - \dot{\varphi}_b\right) \cdot R_b \cdot d}{\nu} \,. \tag{7}$$

In order to describe the following experimental results a modified Reynolds number based on the rotor speed $\dot{\varphi}_R$ is introduced

$$\mathrm{Re}^* = \frac{\left(\dot{\varphi}_R - \dot{\varphi}_b\right) \cdot R_b \cdot d}{\nu} \,. \tag{8}$$

The paper at hand presents a transient modelling approach of an automatic balancing device, which considers the velocity dependent drag coefficient.

3 Experimental Analysis

The test rig, which is modelled in this study and whose run-up is simulated, is depictured in fig. 7. A discoidal rotor is joint on an axis, which is mounted vertically in the stator of an electric motor. The stator itself is mounted by three elastomer bushings, which affect the systems damping and flexibility significantly. The system has an eigenfrequency at $\omega_1 = 50\,\mathrm{rad\,s^{-1}}$ which is related to a translatoric eigenmode orthogonal to the axis of rotation. And a second eigenfrequency at $\omega_2 = 125\,\mathrm{rad\,s^{-1}}$, which is related to a tilting eigenmode orthogonal to the axis of rotation. The conducted experiments use a maximum operation frequency of $\Omega = 70\,\mathrm{rad\,s^{-1}}$, at which a self-balancing effect of the system is expected. In order to reduce the friction force on the ball an outer ring of a ball bearing is used as a race track, see fig. 8. The discoidal rotor is balanced statically in order to set defined unbalance masses into the threads located circumferentially afterwards.

In order to neglect the interaction between multiple balls only one ball with the mass $m_b = 7.6\,\mathrm{g}$ is used whose center is moving on a circular track with a radius of R_b. The mass m_u of the added imbalance is matched, so that the ball can counterbalance this mass exactly. This results in

$$m_u \cdot r_u = (\rho_b - \rho_{fl}) \cdot \frac{\pi d^3}{6} \cdot R_b = 512\,\mathrm{gmm}\,, \tag{9}$$

with ρ_b being the ball density.

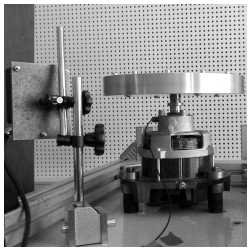

Figure 7: Test rig with the automatic balancing prototype.

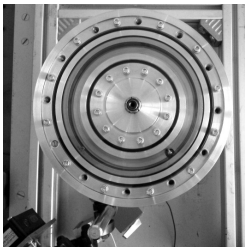

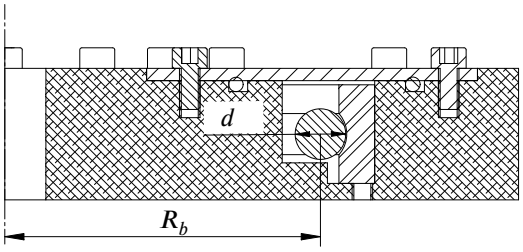

Figure 8: Cross section of the rotor.

With the use of a video camera, which is mounted above the test rig, the position of the rotor and the ball is recorded at 25 frames per second. The corresponding angular velocities, which are shown at the top of fig. 9 can be derived from the footage. It can be seen that the angular velocity of the ball is lagging behind the rotors angular velocity until it reaches the predefined nominal speed. Using equation (8) and the speed difference the Reynolds number can be derived, which is plotted at the bottom of fig. 9.

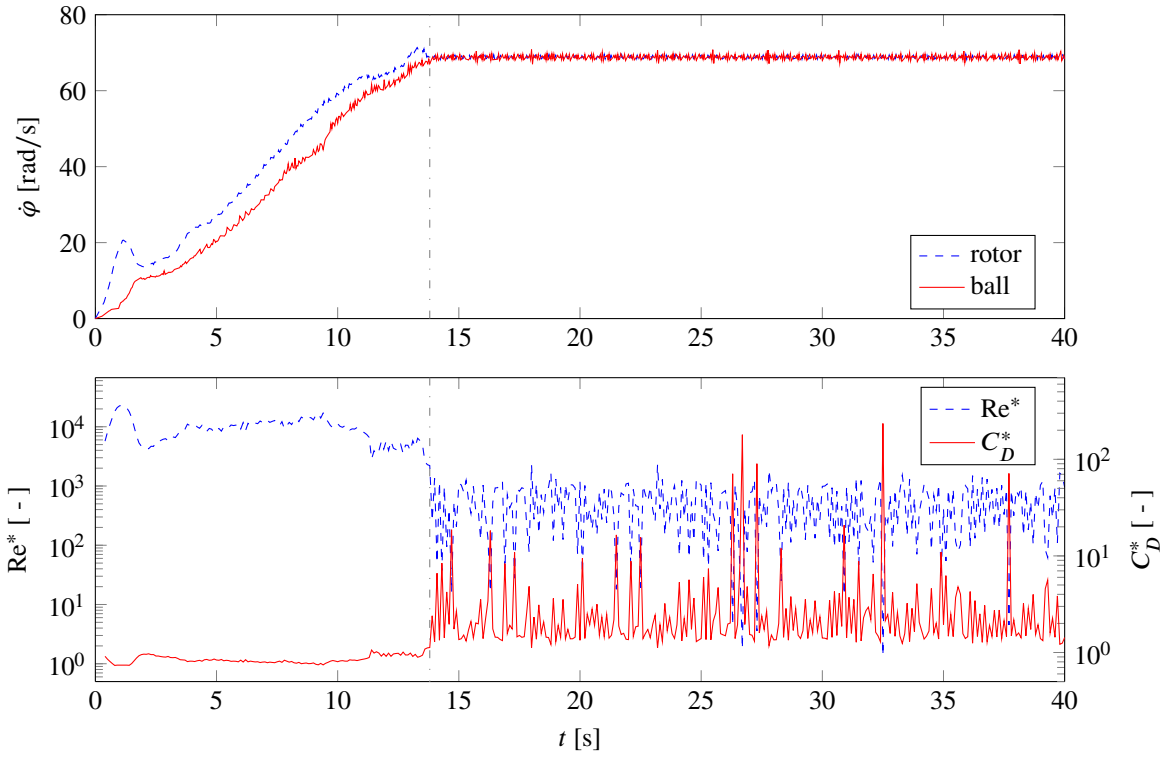

Figure 9: Time dependent quantities of a rotor run-up. Relation $C_D^* = \mathrm{f}(\mathrm{Re}^*)$ corresponding to fig. 10. Fluid properties: $\nu = 0.65\,\mathrm{mm^2 s^{-1}}$, $\rho_{fl} = 760\,\mathrm{kg m^{-3}}$.

Despite the flow velocity being relatively high during the run-up of the rotor, it is reduced in the synchronous phase in which the balls are positioned relative to the imbalance. The dependency of the drag coefficient C_D from the Reynolds number for a free flow around a sphere is well documented in the literature. One empirical approximation from Morrison (2013) is plotted in fig. 10 as a reference. The ball in automatic balancing devices of the described type is in steady contact with the race, which is often designed as a cylindrical surface. Assuming a sufficient large R_b, the flow characteristic can be described by a sphere in contact with a flat surface. Jan and Chen (1997) conducted experimentally that the drag coefficient is increased when considering the wall contact. To achieve this, they examined the terminal velocity of spheres moving down a tilted surface in fluids of different viscosities. The drag coefficient as a function of the Reynolds number is plotted in fig. 10.

Considering this relationship, the drag coefficient C_D^* for the experimental data in fig. 9 can be derived. A significant increase in the drag coefficient can be identified at the start of the positioning phase ($t = 13.8\,\mathrm{s}$). Deviations due to the concave contour of the race are assumed to be negligible. This is supported by studies of Chhabra et al. (2000) on the drag of spheres in tubes, in which it is concluded that the influence of concavity is not significant for

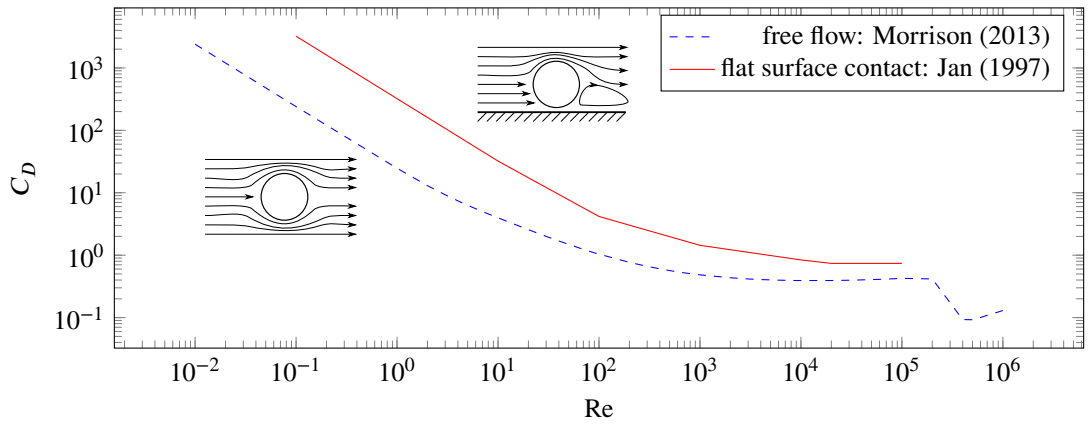

Figure 10: Drag coefficients of flows around spheres.

Reynolds numbers below 4000 and diameter ratios between sphere and tube below 0.5.

Even without knowledge of the exact flow velocity of the fluid the presented data suggest that the drag coefficient underlies high variance during the run-up process of automatic balancing devices. Therefore a significant influence on the balancing characteristic is expected. This influence is examined in the next section with the help of simulation models, which compare the consideration of velocity dependent drag coefficients to the commonly used models.

4 Influence on the Run-up Simulation

The rotor under consideration is modelled in a multi-body simulation program using force elements to represent the interaction between the bodies. The eigenfrequencies are mostly influenced by the bushings, which are modelled by using frequency dependent spring and damper elements. The run-up process is defined by the rotor speed sequence shown in fig. 9. Using a viscosity coefficient of $\beta_{fl} = 720 \times 10^{-6}\,\mathrm{N\,m\,s\,rad^{-1}}$ for equation (5) a good agreement with the experimental record of the ball's velocity is reached in the acceleration phase ($t < 10\,\mathrm{s}$). With an increasing viscosity coefficient the lag between the rotor speed and the ball speed is decreasing.

Based on this model with velocity dependent drag coefficients three additional run-ups with constant drag coefficients C_D are conducted. Firstly, a value of $C_D = 0.74$ is used, which is reached for Reynolds numbers above 10^4 as shown in fig. 10. Secondly, a value of $C_D = 3.7$ is used, which corresponds to the mean value in fig. 9 for $t > 13.8\,\mathrm{s}$. Thirdly, a value of $C_D = 2.0$ in between the prior values is chosen. Fig. 11 shows the effect of the different drag coefficient modelling approaches in the simulation on the ball velocity.

The most obvious disagreement of the simulation results is located in the time interval in which the rotor reaches its nominal speed. In view of the time difference between the rotor reaching its nominal speed and the ball getting synchronous with the rotor[1] the relative and absolute deviations with respect to the reference simulation with velocity dependent drag coefficients are shown in table 1.

This leads to the conclusion that the modelling approach of the drag coefficients has an influence on the dynamics inside the automatic balancing device and should not be neglected, if an optimal choice of the fluid properties is the objective.

Table 1: Time difference in reaching the synchronous motion of the ball with different modelling approaches.

	C_D			
	constant			corresponding
	0.74	2.00	3.70	fig. 10
Δt [s]	4.66	3.10	2.22	3.78
rel. deviation	+23%	-18%	-40%	—

[1]The final point in time at which the relative deviation from the nominal speed is above 1% is used to characterise synchronous motion.

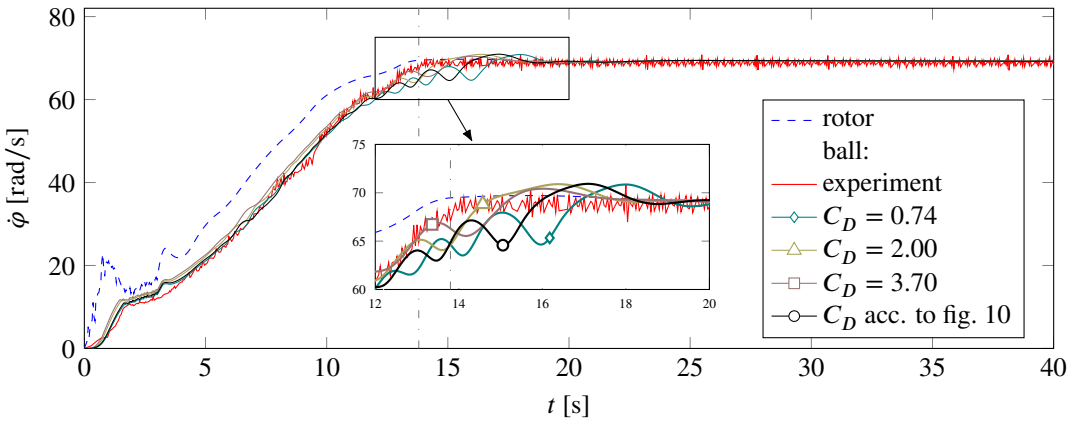

Figure 11: Influence of the drag coefficient model on the ball velocity simulation results.

5 Summary

In the design of automatic balancing devices the choice of fluids shows potential for optimisation. The density and viscosity are influencing the positioning of the counterbalancing mass directly and therefore affecting the rotor vibrations. In particular the reduction of the system-dependent vibration increase at subcritical speeds is to be aimed at.

The modelling of the driving forces on the ball becomes important in simulating the transient process. Previous studies on the influence of friction and virtual mass are implemented in the simulation model. Up to now, the dependence of the drag coefficient from the flow velocity is neglected. The experimental data in section 3 show the variation of the flow conditions during the run-up and provide the motivation to consider the velocity dependency.

Some discrepancy between the simulation and the experimental data of the ball velocity remains in the positioning phase of the ball. It is assumed that the modelled Coulomb friction is not sufficient and the simulation therefore shows oscillatory behaviour of the ball speed. Variation of the friction coefficient μ in reasonable ranges showed little effect, thus a model including rolling friction should be implemented in further research. The effect of neglecting the velocity dependency of drag coefficients is discussed on the basis of simulations in section 4. Despite this restriction the comparison of the different modelling approaches shows a significant influence on the ball velocities and therefore on the transient position of the counterbalancing mass.

The presented study neglects the difference between a flat surface and the curved ball bearing raceway on hand. In addition to that, irregularities in form and position of the mounted raceway are not taken into account leading to remaining differences in the stationary ball positions in comparison to the experimental results. These model enhancements are implemented in future studies. Furthermore, the viscous representation of the fluid acceleration is currently determined by a parametric study in order to reach a good agreement with the experimental data. An alternative based on a priori known quantities, i.e. by solving the Navier-Stokes equations numerically, is to be implemented instead.

6 Future Prospects

For future studies a test rig is planned to validate the curve $C_D = \mathrm{f}(\mathrm{Re})$ as presented by Jan and Chen (1997) for the annulus geometry at hand. Moreover a more accurate model and identification of the friction coefficients is aspired in order to improve the transient simulation. Due to the fact that the acceleration of the fluid is represented by the fitted parameter β_{fl}, numerical solutions will be pursued to get a model on the basis of the annulus geometry, the fluid properties and the rotor acceleration only. The objective is a simulative a priori design of the optimal fluid properties for the automatic balancing device at hand and a subsequent experimental validation.

Acknowledgments

Funded by the German Federal Ministry of Economics and Energy.

References

Benton, E. R.; Clark, A.: Spin-up. *Annu. Rev. Fluid Mech.*, 6, 1, (1974), 257–280.

Chen, H.-W.; Zhang, Q.-J.: Dynamic analysis and design of a balancer for a three-column centrifuge. *Shock and Vibration*, 2016, (2016), 1–13.

Chhabra, R.; Kumar, M.; Prasad, R.: Drag on spheres in rolling motion in inclined smooth tubes filled with incompressible liquids. *Powder technology*, 113, 1, (2000), 114–118.

Green, K.; Friswell, M. I.; Champneys, A. R.; Lieven, N. A.: The stability of automatic ball balancers. In: *IFToMM Seventh International Conference on Rotor Dynamics*, Citeseer (2006).

Huang, W.; Chao, C.; Kang, J.; Sung, C.: The application of ball-type balancers for radial vibration reduction of high-speed optic disk drives. *Journal of Sound and Vibration*, 250, (2002), 415–430.

Ishida, Y.; Matsuura, T.; Zhang, X. L.: Efficiency improvement of an automatic ball balancer. *J. Vib. Acoust.*, 134, 2, (2012), 021012.

Jan, C.-D.; Chen, J.-C.: Movements of a sphere rolling down an inclined plane. *Journal of Hydraulic Research*, 35, 5, (1997), 689–706.

Kim, T.; Na, S.: New automatic ball balancer design to reduce transient-response in rotor system. *Mechanical Systems and Signal Processing*, 37, 1-2, (2013), 265–275.

Majewski, T.: Position error occurrence in self balancers used on rigid rotors of rotating machinery. *Mechanism and Machine Theory*, 23, 1, (1988), 71–78.

Morrison, F. A.: *An introduction to fluid mechanics*. Cambridge University Press (2013).

Ryzhik, B.; Duckstein, H.; Sperling, L.: Automatic balancing of the unsymmetrical rigid rotor. *PAMM*, 2, 1, (2003), 70–71.

Sperling, L.; Ryzhik, B.; Linz, C.; Duckstein, H.: Simulation of two-plane automatic balancing of a rigid rotor. *Mathematics and computers in simulation*, 58, 4, (2002), 351–365.

Thearle, E. L.: Dynamic balancing machine (1936), US Patent 2043845 A.

Address: L. Spannan, C. Daniel, E. Woschke
IFME, Otto-von-Guericke-Universität Magdeburg, Universitätsplatz 2, 39106 Magdeburg, Deutschland
email: {lars.spannan,christian.daniel,elmar.woschke}@ovgu.de